

Influence of Phase Separation on Thermal Conductivity of $\text{Ti}_{1-x}\text{Sn}_x\text{O}_2$ Ceramics

K. Rubenis*, J. Locs, J. Mironova, R. Merijs-Meri

Riga Technical University, Faculty of Material Science and Applied Chemistry, Institute of General Chemical Engineering, Paula Valdena St. 3, LV-1048, Riga, Latvia

received September 15, 2015; received in revised form October 29, 2015; accepted November 3, 2015

Abstract

Many technologically important ceramic materials are made of more than one component. If components are isostructural they can form a stable or a metastable solid solution that can undergo phase separation below a critical temperature, which can significantly affect different properties of the material. In this work, we investigated the effect of phase separation on thermal conductivity at room temperature of $\text{Ti}_{1-x}\text{Sn}_x\text{O}_2$ ceramic with different Ti/Sn ratios. The samples were sintered at 1500 °C and afterwards annealed at 1100 °C for 48 h in order to induce phase separation. It was observed that substitution of Ti with Sn and vice versa considerably reduces the thermal conductivity of the parent phases (TiO_2 and SnO_2). The thermal conductivity of the samples with compositions inside the spinodal region after annealing increased compared with that of samples that had not been annealed while for the compositions outside the spinodal region, only a limited effect was observed.

Keywords: Titanium dioxide, TiO_2 , tin dioxide, SnO_2 , TiO_2 - SnO_2 , phase separation, ceramic, thermal conductivity

I. Introduction

Most technologically important ceramic materials are commonly made of more than one component. The components can form a mixture of different phases or a solid solution if the components involved have the same crystal structure. In many cases, the solid solution is thermodynamically stable only at high temperatures and can undergo phase separation on cooling via nucleation and growth, forming a system where isolated domains of one phase exist in a continuous phase of the other component, or via spinodal decomposition, where sinusoidally varying composition fluctuations are created¹. Phase separation can improve as well as impair different properties of the materials. For example, controlled phase separation can improve the mechanical properties of SiC-AlN and TiN-AlN ceramics^{2,3} or reduce the thermal conductivity and thus enhance the thermoelectric properties of PbTe-GeTe⁴.

Among the metal oxide and non-oxide systems that undergo phase separation, the TiO_2 - SnO_2 system is one of the most commonly investigated. Below a critical temperature of 1430 °C, at critical composition $\text{Ti}_{0.47}\text{Sn}_{0.53}\text{O}_2$, the system possesses an almost symmetrical miscibility gap that widens with decreasing temperature. Phase separation within the miscibility gap generally occurs via spinodal decomposition, resulting in a lamellar structure consisting of alternating TiO_2 - and SnO_2 -rich layers while outside the spinodal decomposition region within the miscibility gap, phase separation occurs via nucleation and

growth⁵. The rate of phase separation in the TiO_2 - SnO_2 system can be controlled with temperature and doping⁶.

Recently, Dynys et al. investigated the thermoelectric properties of doped and undoped $\text{Ti}_{0.75}\text{Sn}_{0.25}\text{O}_2$ ceramic⁷. They suggested that phase separation could be effective in the reduction of thermal conductivity in the TiO_2 - SnO_2 system and could thus improve the thermoelectric properties of this composite.

The objective of this work was to investigate the effect of phase separation on the thermal conductivity at room temperature of $\text{Ti}_{1-x}\text{Sn}_x\text{O}_2$ ceramic samples with different Ti/Sn ratios.

II. Materials and Methods

$\text{Ti}_{1-x}\text{Sn}_x\text{O}_2$, with $x = 0.2, 0.4, 0.6$ and 0.8 were prepared with the sol-gel method. Titanium tetraisopropoxide (TTIP) and tin tetrachloride pentahydrate ($\text{SnCl}_4 \cdot 5\text{H}_2\text{O}$) were used as precursors of Ti and Sn. $\text{SnCl}_4 \cdot 5\text{H}_2\text{O}$ was first dissolved in isopropanol at room temperature. Afterwards, the necessary amount of TTIP required to obtain the predetermined $\text{Ti}_{1-x}\text{Sn}_x\text{O}_2$ composition was added to the $\text{SnCl}_4 \cdot 5\text{H}_2\text{O}$ solution in isopropanol under vigorous stirring. After 30 min of being stirred, the resulting mixture was added drop-wise to HCl-acidified deionized water (pH 1.5). The molar ratio between the metal (Ti + Sn) precursors, isopropanol and water was 1 : 25 : 500 respectively. Finally, the sodium hydroxide solution was added to the obtained mixture until the pH value reached ~4. After 24 hours of aging, the precipitate was collected by means of centrifugation and washed several times with deionized water to remove organic and salt residues. The obtained precipitate was then dried at 100 °C for 24 h and

* Corresponding author: kristaps.rubenis@rtu.lv

calcined at 500 °C for 2 h. After calcination, the obtained material was crushed into a fine powder with mortar and pestle. The obtained powders were uniaxially die-pressed into disc-shaped pellets at 5 MPa pressure, followed by isostatic pressing at 100 MPa pressure. The pressed pellets were sintered at 1500 °C under air conditions for 5 h with heating rate of 2 K/min, followed by natural cooling in the furnace. In order to investigate the effect of phase separation on the thermal conductivity of the samples, the sintered samples were annealed at 1100 °C for 48 h, with a heating and cooling rate of 1.5 K/min.

X-ray diffraction patterns of the calcined $\text{Ti}_{1-x}\text{Sn}_x\text{O}_2$ powders as well sintered and annealed samples were obtained using a PANalytical X'Pert Pro X-ray diffractometer with Cu K_α ($\lambda = 1.5406 \text{ \AA}$) radiation. The morphology of the calcined powders was studied by means of field emission scanning electron microscopy (FE-SEM, TESCAN Mira/LMU). The Brunauer-Emmett-Teller (BET) method was used to determine the specific surface area (SSA) of the calcined $\text{Ti}_{1-x}\text{Sn}_x\text{O}_2$ powders based on N_2 adsorption (Sorptionmeter KELVIN 1042, USA). Densities of the sintered samples were determined according to the Archimedes principle and were related to theoretical densities of the compositions. Specific heat capacity and thermal diffusivity of the sintered and annealed samples were measured with a Netzsch LFA 447 Microflash system. Before the measurement, the samples were coated with graphite on both sides. Afterwards the thermal conductivity of the samples was calculated according to the equation: $k = a\varrho C_p$, where k , a , ϱ and C_p are thermal conductivity, thermal diffusivity, density of the material and heat capacity. The heat capacity of the samples was determined based on comparison with a reference material (Pyroceram). The imprecision of k is estimated to be 10 % for all the samples.

III. Results and Discussion

XRD patterns of the synthesized $\text{Ti}_{1-x}\text{Sn}_x\text{O}_2$ powders after calcination at 500 °C are shown in Fig. 1. Although TiO_2 anatase phase can be stable up to 900 °C⁸, the incorporation of more of a few mol% Sn into the TiO_2 lattice promotes transformation of anatase to rutile already at 200 °C⁹. After calcination at 500 °C, only diffraction peaks corresponding to the rutile phase were observed for all synthesized compositions, including the Ti-rich samples. With increasing Sn content in the synthesized $\text{Ti}_{1-x}\text{Sn}_x\text{O}_2$ powders, the diffraction peak positions shift from positions characteristic of rutile TiO_2 (JCPDS card 75–1753) towards positions characteristic of the rutile phase of SnO_2 (JCPDS card 01–077–0447).

SEM micrographs of the synthesized $\text{Ti}_{1-x}\text{Sn}_x\text{O}_2$ powders after calcination at 500 °C are shown in Fig. 2. It can be observed that all $\text{Ti}_{1-x}\text{Sn}_x\text{O}_2$ powders consist of highly agglomerated particles with dimensions in the nanometer range <100 nm. The SSA of the calcined powders as determined with the BET method was 87.33 g/m² for $\text{Ti}_{0.8}\text{Sn}_{0.2}\text{O}_2$, 82.88 g/m² for $\text{Ti}_{0.6}\text{Sn}_{0.4}\text{O}_2$, 86.72 g/m² for $\text{Ti}_{0.4}\text{Sn}_{0.6}\text{O}_2$ and 72.8 g/m² for $\text{Ti}_{0.2}\text{Sn}_{0.8}\text{O}_2$ respectively.

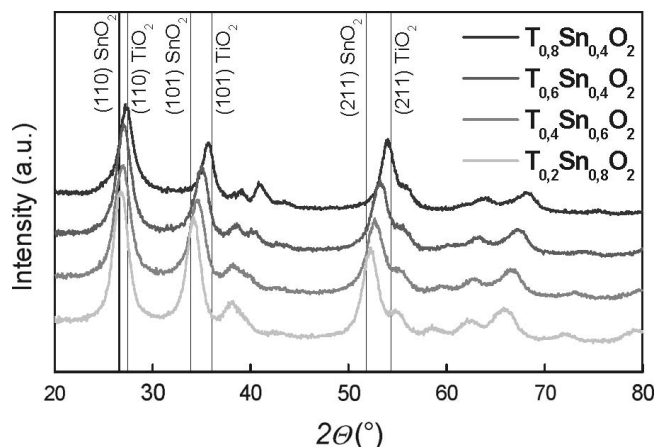


Fig. 1: XRD patterns of the $\text{Ti}_{1-x}\text{Sn}_x\text{O}_2$ powders calcined at 500 °C.

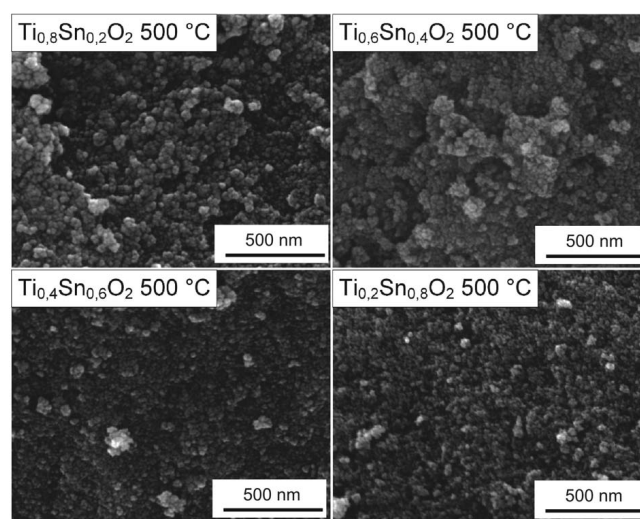


Fig. 2: SEM micrographs of the calcined $\text{Ti}_{1-x}\text{Sn}_x\text{O}_2$ powders.

Density of the samples after sintering at 1500 °C increased with increasing Sn content and was 93 % for $\text{Ti}_{0.8}\text{Sn}_{0.2}\text{O}_2$, 94 % for $\text{Ti}_{0.6}\text{Sn}_{0.4}\text{O}_2$, 96 % for $\text{Ti}_{0.4}\text{Sn}_{0.6}\text{O}_2$ and 97 % of theoretical density for $\text{Ti}_{0.2}\text{Sn}_{0.8}\text{O}_2$. The density of the samples did not change during the annealing process. XRD patterns of $\text{Ti}_{1-x}\text{Sn}_x\text{O}_2$ ceramic after sintering at 1500 °C and the subsequent annealing at 1100 °C for 48 h are shown in Fig. 3.

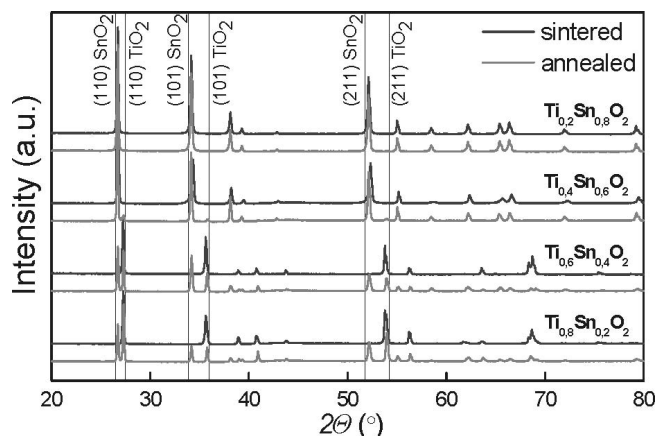


Fig. 3: XRD patterns of $\text{Ti}_{1-x}\text{Sn}_x\text{O}_2$ samples after sintering at 1500 °C and annealing at 1100 °C for 48 h.

Owing to the relatively low cooling rate after the sintering process, the XRD patterns of the sintered $Ti_{1-x}Sn_xO_2$ samples exhibit minor indications of phase separation for some of the $Ti_{1-x}Sn_xO_2$ compositions. Similar to the calcined $Ti_{1-x}Sn_xO_2$ powders, diffraction peaks shift to lower angles with increasing Sn content in the sintered samples, which can be attributed to the differences in the effective ionic radii of Ti^{4+} and Sn^{4+} . Since Sn^{4+} has larger ionic radii than Ti^{4+} , substitution of Ti^{4+} with Sn^{4+} causes an increase in the lattice parameters, which shifts the diffraction peaks to lower angles. As can be observed from the diffraction patterns, annealing of the sintered $Ti_{1-x}Sn_xO_2$ samples at 1100 °C for 48 h enhances the phase separation process. Peak splitting and the appearance of new peaks can be observed in the diffraction patterns for all annealed samples except the sample with a composition of $Ti_{0.2}Sn_{0.8}O_2$. The newly formed peaks were identified as corresponding to rutile TiO_2 and rutile SnO_2 phases. The reason why phase separation was not observed in the case of $Ti_{0.2}Sn_{0.8}O_2$ could be related to the slower decomposition rate within the nucleation and growth region¹⁰, since the chosen annealing temperature for samples $Ti_{0.8}Sn_{0.2}O_2$ and $Ti_{0.2}Sn_{0.8}O_2$ is in the nucleation and growth region while for samples $Ti_{0.4}Sn_{0.6}O_2$ and $Ti_{0.6}Sn_{0.4}O_2$ in the spinodal region⁵.

The thermal conductivity at room temperature of the sintered $Ti_{1-x}Sn_xO_2$ samples before and after annealing at 1100 °C is shown in Fig. 4.

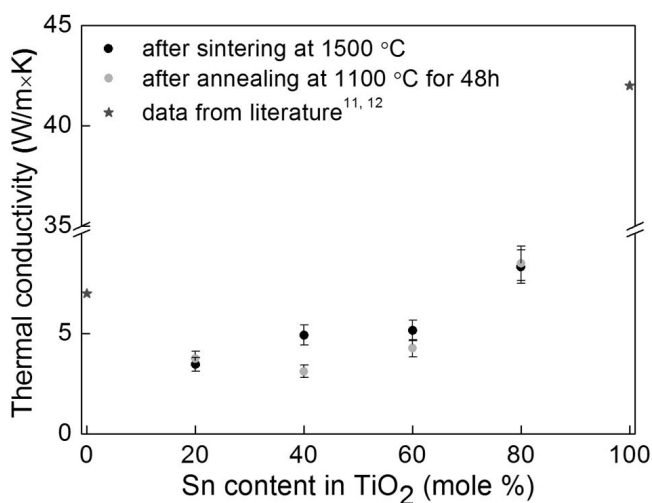


Fig. 4: Thermal conductivity at room temperature for $Ti_{1-x}Sn_xO_2$ samples after sintering and annealing.

As can be seen from Fig. 4, substitution of Ti with Sn and vice versa significantly reduces the thermal conductivity of the parent phases. Since Ti and Sn possess large differences in atomic mass, the reduced thermal conductivity after sintering of $Ti_{1-x}Sn_xO_2$ compounds can be mainly attributed to mass-difference scattering mechanism. After sintering at 1500 °C, the lowest values of thermal conductivity are exhibited by $Ti_{1-x}Sn_xO_2$ compositions close to the equimolar Ti and Sn ratio. It was observed that annealing considerably affects the thermal conductivity of the samples. The thermal conductivity of samples with composition $Ti_{0.8}Sn_{0.2}O_2$ and $Ti_{0.2}Sn_{0.8}O_2$ was not much affected while for the samples $Ti_{0.6}Sn_{0.4}O_2$ and $Ti_{0.4}Sn_{0.6}O_2$, thermal conductivity increased as compared with that of

the unannealed samples. Differences in the thermal conductivity of the annealed and unannealed samples could be attributed to a change in the phonon scattering mechanism. Phonon scattering owing to the mass-difference scattering mechanism is most effective when elements that form a solid solution are distributed randomly and uniformly throughout the solid. During phase separation, the $Ti_{1-x}Sn_xO_2$ solid solution decomposes, forming Ti-rich and Sn-rich regions. As a result, phonon scattering owing to the mass-difference mechanism decreases while interface scattering becomes a dominant scattering mechanism⁴. Interface scattering is most effective when the material contains a high density of interfaces. Probably owing to the long annealing time in spinodal region (samples $Ti_{0.6}Sn_{0.4}O_2$ and $Ti_{0.4}Sn_{0.6}O_2$), Ti- and Sn-rich regions grow in size, thus reducing interface density, which could lead to increased thermal conductivity as compared with that of unannealed samples. Since decomposition in the nucleation and growth region (samples with composition $Ti_{0.8}Sn_{0.2}O_2$ and $Ti_{0.2}Sn_{0.8}O_2$) is slower than in the spinodal region, probably, with the annealing process at the chosen temperature and time, the interface density does not change much and thermal conductivity of these samples is not substantially affected, as compared with that of the unannealed samples.

IV. Conclusions

In this work, the effect of phase separation on the thermal conductivity of the TiO_2 - SnO_2 system was investigated. It was observed that substitution of Ti with Sn and vice versa significantly reduces the thermal conductivity of the parent phases. The chosen annealing conditions caused an increase in thermal conductivity for samples annealed in the spinodal region while for the samples annealed in the nucleation and growth region, thermal conductivity was not substantially affected compared with that of the unannealed samples.

Acknowledgement

This work has been supported by the National Research Programme No. 2014.10-4/VPP-3/21 “Multifunctional Materials and composites, photonicS and nanotechnology (IMIS2)”.

References

- Harper, C.A. (ed.): Handbook of ceramics, glasses and diamonds. McGraw-Hill, New York, 2001.
- Miura, M., Yogo, T., Hirano, S.I.: Phase separation and toughening of SiC-AlN solid-solution ceramic, *J. Mater. Sci.*, **28**, 3859–3865, (1993).
- Knutsson, A., Johansson, M.P., Karlsson, L., Odén, M.: Thermally enhanced mechanical properties of arc evaporated $Ti_{0.34}Al_{0.66}N/TiN$ multilayer coatings, *J. Appl. Phys.*, **108**, 044312:1–044312:7, (2010).
- Gorsse, S., Bauer Pereira, P., Decourt, R., Sellier, E.: Microstructure engineering design for thermoelectric materials: An approach to minimise thermal diffusivity, *Chem. Mater.*, **22**, [3], 988–993, (2010).
- Park, M.W., Mitchell, T.E., Heuer, A.H.: Subsolidus equilibria in the TiO_2 - SnO_2 system, *J. Am. Ceram. Soc.*, **58**, 44–47, (1975).

- 6 Chaisan, W., Yimnirun, R., Ananta, S., Cann, D.P.: The effects of the spinodal microstructure on the electrical properties of $\text{TiO}_2\text{-SnO}_2$ ceramic, *J. Solid State Chem.*, **178**, 613–620, (2005).
- 7 Dynys, F.W., Berger, M.H., Sehirlioglu, A.: Thermoelectric properties of undoped and doped $(\text{Ti}_{0.75}\text{Sn}_{0.25})\text{O}_2$, *J. Am. Ceram. Soc.*, **95**, 619–626, (2012).
- 8 Etacheri, V., Seery, M.K., Hinder, S.J., Pillai, S.C.: Oxygen rich titania: A dopant free, high temperature stable, and visible-light active anatase photocatalyst, *Adv. Funct. Mater.*, **21**, 3744–3752, (2011).
- 9 Fu, G., Yang, Y., Wei, G., Shu, X., Qiao, N., Deng, L.: Influence of Sn doping on phase transformation and crystallite growth of TiO_2 nanocrystals, *J. Nanomater.*, **2014**, [1], 835450:1–5, (2014).
- 10 Park, M.W., Mitchell, T.E., Heuer, A.H.: Decomposition of $\text{TiO}_2\text{-SnO}_2$ solid solutions, *J. Mater. Sci.*, **11**, 1227–1238, (1976).
- 11 Fayette, S., Smith, D.S., Smith, A., Martin, C.: Influence of grain size on thermal conductivity of tin oxide ceramics, *J. Eur. Ceram. Soc.*, **20**, 297–302, (2000).
- 12 Samsonov, G.V.: The oxide handbook, IFI/Plenum Press, New York, 1982.